

## Controlled Modification of Individual Adsorbate Electronic Structure

J. Kliewer and R. Berndt\*

*RWTH Aachen, 2. Physikalisches Institut, D-52056 Aachen, Germany  
and Institut für Experimentelle und Angewandte Physik, Christian-Albrechts-Universität zu Kiel,  
D-24098 Kiel, Germany*

S. Crampin†

*Department of Physics, University of Bath, Bath BA2 7AY, United Kingdom  
(Received 21 June 2000)*

Modification of the electronic structure of a single Mn adsorbate placed within a geometrical array of adatoms on Ag(111) is observed using local spectroscopy with the scanning tunneling microscope. The changes result from coupling between the adsorbate level and surface electronic states of the substrate. These surface states are scattered coherently within the adatom array, mediating the presence and shape of the array to the adsorbate within. The dimension and geometry of the adatom array thus provide a degree of control over the induced changes.

PACS numbers: 73.20.At, 61.16.Ch, 72.10.Fk, 73.20.Dx

One of the aims of nanoscale science is to accomplish the local modification of material properties on a nanometer scale. Using the scanning tunneling microscope (STM) it is possible to maneuver individual atoms on a surface, thereby controlling structure on an atomic dimension. Through the artificial synthesis of nanoscale structures it has also become possible to modify surface electronic structure, as has been demonstrated through characterization by scanning tunneling spectroscopy [1–4]. Here we demonstrate control over the electronic structure of an individual adsorbate, by manipulating locally the substrate electronic structure to which it couples. This may open up the possibility of atomic control over magnetic and chemical properties.

The basic mechanism of our approach may be understood within the framework of Newns' model Hamiltonian describing a single adsorbate level interacting with a surface [5]:

$$H = \sum_k \epsilon_k c_k^\dagger c_k + \epsilon_a d_a^\dagger d_a + \sum_k (U_{ka} d_a^\dagger c_k + \text{H.c.}). \quad (1)$$

$c_k^\dagger/c_k$  are creation/annihilation operators for eigenstates  $k$  of the substrate with energy  $\epsilon_k$ , and  $d_a^\dagger/d_a$  and  $\epsilon_a$  are the corresponding terms for the adsorbate level, and  $U_{ka}$  describes the hybridization between the substrate and adsorbate states. This system may be solved via the Dyson equation, yielding the contribution of the adsorbate to the local density of electronic states (LDOS) at an energy  $\omega$  outside the surface as

$$n(\mathbf{r}, \omega) = -\frac{1}{\pi} \text{Im} \frac{|\Psi_a(\mathbf{r})|^2}{\omega - \epsilon_a - \Sigma(\omega)}, \quad (2)$$

where  $\Psi_a$  is the adsorbate wave function. The imaginary part of the self-energy-like term  $\Sigma = \Lambda - i\Gamma$  is a weighted density of states

$$\Gamma(\omega) = \pi \sum_k |U_{ka}|^2 \delta(\omega - \epsilon_k) \quad (3)$$

and  $\Lambda(\omega)$  its Hilbert transform. Replacing  $|U_{ka}|^2$  by its average value gives  $\Gamma(\omega) \simeq \pi \langle U^2 \rangle n_s(\omega)$ , where  $n_s$  is the density of states of the surface in the absence of the adsorbate. Thus by controlling  $n_s$  one may exert a degree of control over the adsorbate electronic structure.

There is a certain class of systems where control of  $n_s$  is readily accomplished. These are the (111) faces of the noble metals, at which electrons in surface states make a sizable contribution to the LDOS immediately outside the surface where an adsorbate sits, at energies close to the Fermi level. Through lateral confinement within artificial structures, both the energetics and the spatial distribution of these surface state electrons may be controllably varied. While  $n_s$  is conventionally assumed to be rather featureless and thus causes a mere shift and broadening of the adsorbate level, in the present case of quantum constructions  $n_s$  displays rich structure giving rise to unexpected modification of the adsorbate LDOS.

Figure 1 shows a nanoscale structure in which the properties of these surface state electrons are modified. This surface nanocavity has been constructed in a custom-built ultrahigh vacuum (UHV) STM [6] operating at a temperature of  $T = 4.6$  K, from Mn atoms that were evaporated onto the cold Ag(111) substrate, previously prepared by repeated sputter-anneal cycles in UHV. Scans with the STM were used to identify a region of the surface free from steps and other defects, where the nanocavity was constructed, although small amounts of defects within the cavity did not affect the essential observation. We verified that the structures were stable during acquisition of differential conductivity ( $dI/dV$ ) spectra. Atom manipulation was achieved by lowering the STM tip (electrochemically etched Ir, W, or Nb, *in vacuo* treated by heating and ion bombardment) above a Mn adatom (sample bias

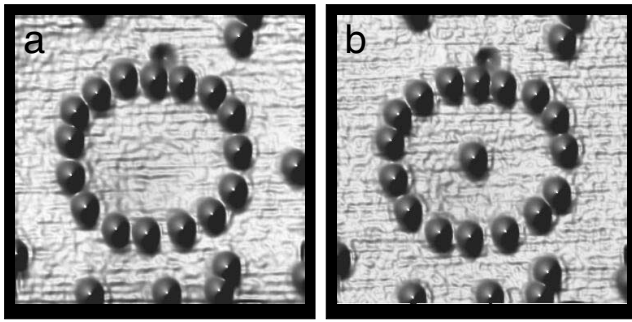


FIG. 1. STM constant current topographs of a 16 atom array of Mn adatoms on Ag(111) (scan size  $160 \times 160 \text{ \AA}^2$ ,  $V = 1 \text{ V}$ ,  $I = 0.1 \text{ nA}$ ). (a) before and (b) after the insertion of a Mn atom into the center.

$V = 3 \text{ V}$ , tunneling current  $I = 6 \text{ nA}$ ) and then moving it slowly (one lattice constant per second) to the desired location, with progress monitored by feeding the current signal through an audio amplifier—atom jumps from adsorption site to adsorption site caused sudden changes in tip-sample separation, resulting in sharp changes in tunnel current. Once the adatom had reached the desired spot the tip was retracted and a scan was performed to check the position. Assembling a 35 atom ring took approximately one hour.

Structures such as these support nanocavity modes at energies dictated by the geometry. We characterize their electronic properties through differential conductivity ( $dI/dV$ ) measurements taken with the STM, which are closely related to the LDOS at the surface beneath the STM tip.

Figure 2 (spectra labeled 1) shows  $dI/dV$  spectra [7] from the empty nanocavities displayed in Figs. 1, 2d, and 2e. The spectral peaks correspond to the energy levels of the confined surface state electrons [1], and occur at energies related to the eigenvalues of the Helmholtz equation  $(\nabla^2 + k^2)\psi = 0$  for the two-dimensional cavity through  $E_n = E_0 + \hbar^2 k_n^2 / 2m^*$ , where  $n = 1, 2, \dots$  labels the states with finite spectral weight  $|\psi(x, y)|^2$  at the lateral position of the STM tip, and  $E_0$  and  $m^*$  are the binding energy and effective mass of the surface state on clean Ag(111),  $-67 \text{ meV}$  and  $0.4$ , respectively. The envelope of the spectra results from single-particle scattering processes [8,9], electron-electron and electron-phonon interactions [10], and instrumental effects that broaden the levels into resonances. A full account of the electronic structure of a large number of nanocavities that we have investigated will be published elsewhere [11].

This strongly varying surface LDOS results in a structure in  $\Sigma(\omega)$  that gives rise to a modified adsorbate electronic structure, Eq. (2). In Fig. 2 (spectra labeled 2) we display the differential conductivity of single Mn atoms placed at the centers of the nanocavities. The spectra are characterized by a number of dips, with a distribution and envelope that mimics the original spectrum on the empty nanocavity, but with peaks lining up with troughs and vice versa. Although on occasion as a result of the introduction of the Mn there was a change in the location of one or more atoms forming the outer boundary, the reversed “contrast” in the tunneling spectra cannot be attributed to this as similar changes to empty structures have a negligible

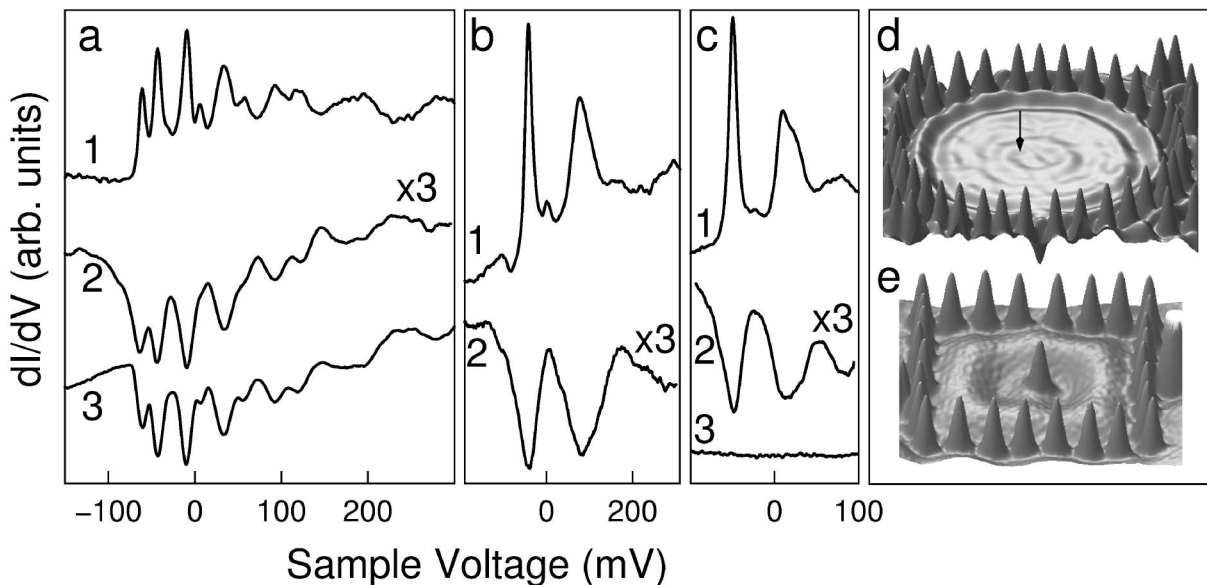


FIG. 2.  $dI/dV$  spectra of nanocavities without (spectra 1) and with (spectra 2) central Mn atoms recorded from (a) 35 Mn atom ring of radius  $\sim 115 \text{ \AA}$ , (b) 16 atom ring of Fig. 1, (c) 28 atom rectangle, sides  $\sim 90 \times 100 \text{ \AA}^2$ . (d) STM image of the empty ring (a), spectra taken at the position marked by an arrow. (e) STM image of the filled rectangle (c). The relationship between the electronic structure of the empty nanocavity and that of the adsorbate introduced into it is apparent from spectrum 3 in (a), where the  $dI/dV$  spectrum of the empty cavity has been inverted and scaled, reproducing the spectral features on the adsorbate. Spectrum 3 in (c) shows a  $dI/dV$  spectrum of a Mn atom close to a step which is not in a cavity.

effect on the spectrum recorded in the middle. Furthermore, we have observed qualitatively similar behavior in a number of nanocavities of different sizes and shapes including random arrays. We can also dismiss the possibility of the effect resulting from some mechanism involving the tip electronic structure. All STM images were obtained using tips that were treated until single atoms imaged as round bumps on the surface, with Ir, W, and Nb tips giving comparable results.

Mn on Ag(111) exists in a high-spin state (moment  $\sim 4.5\mu_B$ ), and at these temperatures and over a comparable voltage range a Mn atom on an otherwise clean Ag(111) surface appears electronically featureless in tunneling spectroscopy (Fig. 2c, spectrum 3), with  $dI/dV$  only rising sharply for voltages above 2 eV when tunneling into unoccupied minority spin Mn  $d$  levels becomes possible [12]. To confirm that the structure in Fig. 2 is a direct consequence of the Mn residing within the nanocavity, and to exclude possible exotic spin effects [13–15], we have also performed electronic structure calculations on a nanocavity on Ag(111), using multiple-scattering methods that have been successfully employed in previous studies of Fe corrals on Cu(111) [10] and Ag islands on Ag(111) [3]. These calculations determine the single-particle Green function from the scattering properties of the individual atoms. Initially the Green function for the surface of a *semi-infinite* Ag(111) crystal is calculated, thereby ensuring that there are no spurious spectral features associated with size quantization, such as arise when the thin film or supercell approximation is made. The Mn atoms of the ring plus any central atom are subsequently included as a perturbation treated exactly to all orders.

In Fig. 3a we compare the LDOS of (spectrum 1) the center of an empty ring of 35 Mn atoms (radius  $\sim 115 \text{ \AA}$ ) with (spectrum 2) a Mn atom at the center of this ring [16]. The calculations reproduce the “reversed contrast” structure within the Mn spectrum, in good agreement with the experiment (Fig. 2a), thereby confirming our interpretation. Calculations for the smaller 16 atom ring (Fig. 3b) and the rectangular array (Fig. 3c) also display spectral structure consistent with experiment, and taken together our results demonstrate that the spectral features on a Mn adatom are influenced by the nature of the cavity within which it resides.

The inverted structure is characteristic of a strongly coupled adsorbate level, with  $\Sigma(\omega)$  dominating the denominator in Eq. (2) so that the structure in  $n(\omega)$  is related to the Hilbert transform of  $n_s(\omega)$ , which oscillates as  $n_s(\omega)$  oscillates. The connection between the two is most clearly seen in Fig. 2a where the differential conductivity on the adsorbate (spectrum 2) is reproduced from the clean surface spectrum (spectrum 3). We can report experimental observations of related modified adsorbate electronic structure in other systems, including Mn dimers, and have seen similar effects in calculations on Fe adatoms in Fe rings on Cu(111). In the present system the relevant level is the Mn  $s$  state, as shown by the orbital decomposition of the LDOS found in the electronic structure calculations, Fig. 3a.

Our results provide the first demonstration that the electronic structure of an adsorbate can be modified through *geometrical* control of surface state wave functions, by varying the shape of a nanocavity in which the adsorbate is positioned. We note there are other possibilities that have yet to be fully investigated, which could enhance the extent

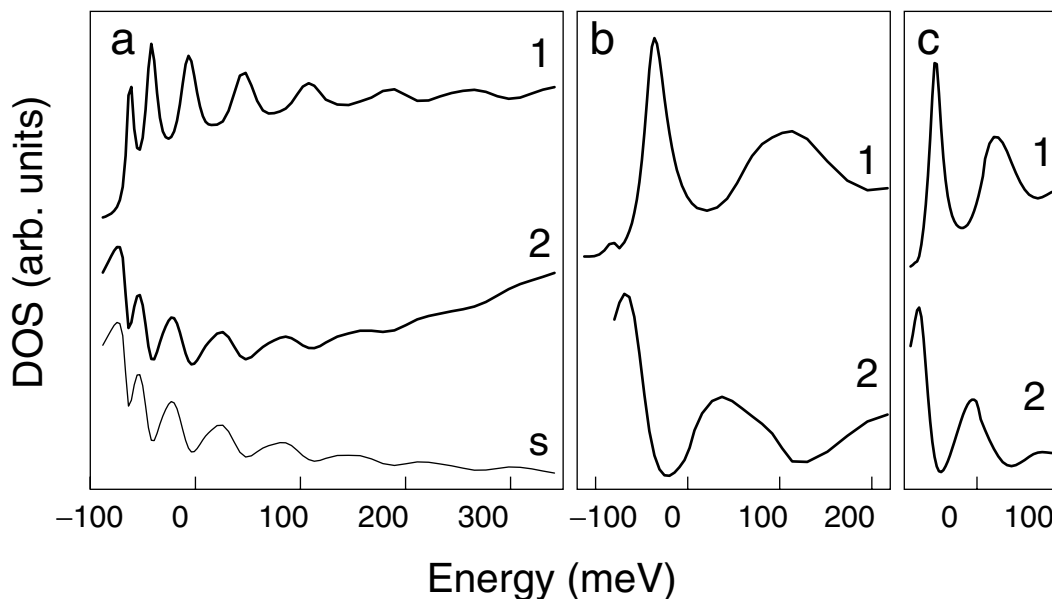


FIG. 3. LDOS integrated through a  $17 \text{ \AA}^3$  spherical volume centered at the middle of Mn structures on Ag(111). Spectra 1 and 2 correspond to structures without and with a central atom. (a) 35 Mn atom ring, (b) 16 atom ring, (c) 28 atom rectangle. In (a), the  $s$  component of the LDOS is indicated.

to which the cavity electronic structure is tailored, so, for example, enabling a single resonant mode to be selected within a desired energy range. In such a scenario, it would be possible to selectively interact with specific adsorbate levels. A natural possibility is to vary the species from which the confining barrier is constructed, although to date there is only limited evidence that this has a significant effect [10]. However, monatomic steps on Au(111) comprised of {100} or {111} microfacets have been observed to scatter differently surface electrons [17], indicating that there is scope for influencing the properties of nanocavities by varying the internal structure of their outer boundaries [18]. Furthermore, the design of semiconductor heterostructures and photonic band gap materials widely exploits the dramatic changes in scattering properties that arise when scatterers are arranged periodically at intervals similar to the wavelength. Here nanocavities constructed from concentric rings or boxes of adatoms may provide the optimum in customization. Finally, we note that the energy dispersion of the surface state electrons is modified through alloying [19], and as a result of strain in thin film overlayers [20], both of which can also be used to control the spectrum of nanocavity modes.

To summarize, we report the controlled modification of the electronic structure on a single Mn adsorbate. This modification was achieved by placing the Mn atom within geometrical arrays of adatoms on Ag(111), and observed with local tunneling spectroscopy. The changes result from the coupling between the Mn  $s$  level and surface electronic states of the substrate, which are strongly influenced by the size and geometry of the nanocavity.

J.K. and R.B. acknowledge the support of the Forschungsverbund Nanowissenschaften NRW and the DFG via SFB 341. S.C. acknowledges the support of the EPSRC.

---

\*Author to whom correspondence should be addressed.

Email address: berndt@physik.uni-kiel.de

†Email address: s.crampin@bath.ac.uk

[1] M.F. Crommie, C.P. Lutz, and D.M. Eigler, *Science* **262**, 218 (1993).

- [2] Ph. Avouris and I.-W. Lyo, *Science* **264**, 942 (1994).  
 [3] J. Li, W.-D. Schneider, R. Berndt, and S. Crampin, *Phys. Rev. Lett.* **80**, 3332 (1998).  
 [4] L. Bürgi, O. Jeandupeux, A. Hirstein, H. Brune, and K. Kern, *Phys. Rev. Lett.* **81**, 5370 (1998).  
 [5] D.M. Newns, *Phys. Rev.* **178**, 1123 (1969).  
 [6] J. Kliewer, Ph.D. thesis, RWTH–Aachen, 2000 (to be published).  
 [7]  $dI/dV$  spectra were recorded under open feedback loop conditions using a lock-in amplifier with modulation voltages of 0.8–5 mV<sub>rms</sub> added to the sample bias.  
 [8] E.J. Heller, M.F. Crommie, C.P. Lutz, and D.M. Eigler, *Nature (London)* **369**, 464 (1994).  
 [9] S. Crampin, M.H. Boon, and J.E. Inglesfield, *Phys. Rev. Lett.* **73**, 1015 (1994).  
 [10] S. Crampin and O.R. Bryant, *Phys. Rev. B* **54**, R17367 (1996).  
 [11] J. Kliewer *et al.* (unpublished).  
 [12] D. van der Marel, C. Westra, G.A. Sawatzky, and F.U. Hillebrecht, *Phys. Rev. B* **31**, 1936 (1985).  
 [13] J. Li, W.-D. Schneider, R. Berndt, and B. Delley, *Phys. Rev. Lett.* **80**, 2893 (1998).  
 [14] V. Madhavan, W. Chen, T. Jamneala, M.F. Crommie, and N.S. Wingreen, *Science* **280**, 567 (1998).  
 [15] H.C. Manoharan, C.P. Lutz, and D.M. Eigler, *Nature (London)* **403**, 512 (2000).  
 [16] Our calculations employ the atomic sphere approximation, use partial waves up to  $\ell = 4$ , and 19  $g$  vectors in the  $2d$  plane wave basis. Brillouin zone integrals are performed using a special direction method, with special attention paid to the near singular structure at the surface state wave vector. Fully self-consistent calculations on the Ag(111) surface are performed, giving a work function  $\Phi = 4.56$  eV, surface state binding energy  $E_0 = -72$  meV, and effective mass  $m^* = 0.37$ . The potentials used in the Mn array calculations are taken from self-consistent calculations for dilute Mn overlayers. Our results are robust with respect to reasonable variations in the Mn potentials, so that the use of the atomic sphere approximation is not significant.  
 [17] Y. Hasegawa and P. Avouris, *Phys. Rev. Lett.* **71**, 1071 (1993).  
 [18] Similar steps on Ag(111) do not exhibit different scattering properties though [4].  
 [19] R. Prasad, A.Y. Serageldin, and A. Bansil, *J. Phys. Condens. Matter* **3**, 801 (1991).  
 [20] G. Neuhold and K. Horn, *Phys. Rev. Lett.* **78**, 1327 (1997).